Multiband open-ended resonant antenna based on one ECRLH unit cell structure

Gao, Xiang; Jackson, Timothy; Gardner, Peter

DOI:
10.1109/LAWP.2016.2632299

Multiband Open-Ended Resonant Antenna Based On One ECRLH Unit Cell Structure

X. Gao, T. J. Jackson, and P. Gardner, *Senior Member, IEEE*

***Abstract*—In this letter, a microstrip-fed open-ended resonant antenna (RA) based on an extended composite right/left-handed (ECRLH) unit cell structure is presented for multiband operations. This antenna includes an asymmetric ECRLH unit cell as the main resonator and a short microstrip line as the feeding line. This designed RA, of overall size of 56 mm × 64 mm × 1.575 mm, generates ten operating resonances covering several commercial frequency bands over 0.5-6 GHz. Measured and simulated results have a close agreement. Furthermore, the equivalent circuit model of the proposed RA is developed. For each operating resonance, the major control parts in this antenna structure and the primary radiation sources for each operating resonance are analyzed and summarized.**

***Index Terms*—Extended composite right/left-handed (ECRLH), multiband antenna, resonant antenna.**

I. Introduction

WITHIN the last decade, artificial electromagnetic metamaterial has attracted great interest due to the design possibilities enabled by non-linear dispersion, simultaneous negative electric permittivity and magnetic permeability, backward-wave propagation, and negative refractive index. Composite right/left-handed (CRLH) transmission-line (TL) structures are a classic artificial electromagnetic metamaterial, which have already been used in designs for microwave, millimeter-wave and optical components [1]-[3]. CRLH unit cells can also be combined with conventional antennas to realize metamaterial-inspired resonant antennas (RAs) [4]-[6]. These RAs can be categorized into two types – short-ended and open-ended. In short-ended RAs, one or more CRLH unit cells are integrated into conventional antennas with a short circuit at the termination, enabling the RAs to operate in different modes, i.e., the zeroth-order mode (*m=0*), negative-order modes (*m=-1,-2,-3,…*), or positive-order modes (*m=+1,+2,+3,…*). Most RAs of this type are designed to radiate using the zeroth-order mode, as in [4] and [5]. In open-ended RAs, the major advantage is that more operating resonances can be generated for multiband applications by usually exciting one CRLH unit cell. In [6], a monopole antenna loaded with one CRLH unit cell was proposed for triple-band applications. In all these designs, only two or three resonances are generally generated to work at the chosen frequency bands.

Multiband property can be achieved by the extended CRLH (ECRLH) TL structure [7] which is also referred to as the generalized negative-refractive-index (GNRI) TL structure [8]. The equivalent circuit model of one ECRLH TL unit cell structure is shown in Fig. 1. With four pairs of L-C resonators, the ECRLH TL unit cell structure can generate two pairs of the alternating left-handed (LH) and right-handed (RH) bands, thereby forming dual, triple, quad or even multiple bands in different operating conditions. In [9], a distributed amplifier for quad-band applications was designed based on the ECRLH TL structure. In [10], a substrate integrated waveguide periodic leaky wave antenna based on the ECRLH TL structure was designed for dual-band applications with the filtering characteristics achieved simultaneously. The ECRLH unit cell structure can also be used for RA designs to achieve multiband operations.

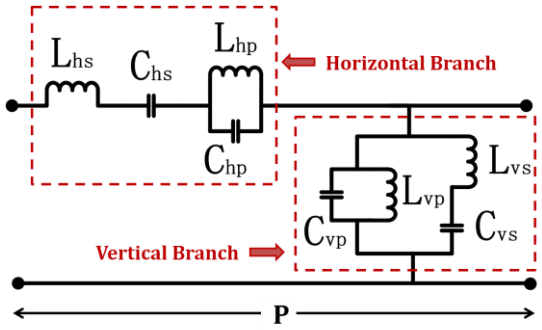

Fig. 1. Equivalent circuit model of one asymmetric ECRLH unit cell.

This letter presents a microstrip-fed open-ended RA incorporating an asymmetric ECRLH unit cell for multiband operation. The configurations of the proposed RA are shown in Fig. 2. In this RA, three interdigital structures (IDSs) are designed to realize C_{hs}, C_{hp}, and C_{vs}, respectively. Fig. 3 shows these three IDSs with different dimensions. The proposed RA generates ten operating resonances over 0.5-6 GHz using the intrinsic modes of the ECRLH unit cell resonant structure. This antenna is fabricated and measured to demonstrate the antenna characteristics. The equivalent circuit model of this RA is also developed. Furthermore, the major control parts in the RA structure and the primary radiation sources for each operating resonance are analyzed and summarized.

II. ECRLH TL Theory

The ECRLH TL theory, which has been explained in [7] and [8], is briefly introduced here. The ECRLH TL structure can have two CRLH bands respectively at the low and high frequencies with separation by a middle bandgap. Referring to

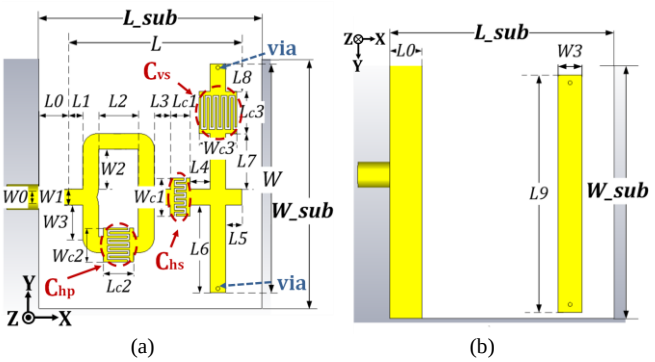

Fig. 2. Configurations of the proposed RA, (a) front view; (b) rear view.

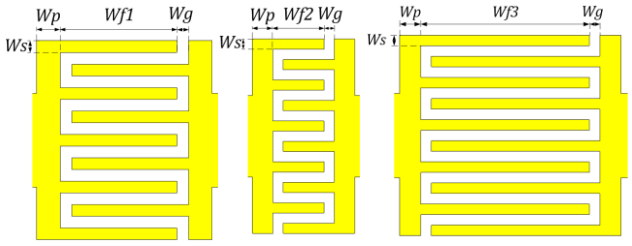

Fig. 3. IDSs in the RA structure, (a) C_{hp}; (b) C_{hs}; (c) C_{vs}.

TABLE I
DIMENSIONS OF THE PROPOSED RA

Symbol	Dimension (mm)	Symbol	Dimension (mm)
L_sub	56	*W_sub*	64
L	43	*W*	57.5
L0	8	*W0*	3
L1	3	*W1*	4
L2	5	*W2*	10
L3, L5	4	*W3*	8
L4	5	*W4*	6
L6	22	*Wp*	1
L7	14	*Wg, Ws*	0.5
L8	7	*Wf1*	5
L9	59.5	*Wf2*	2.5
Lc1	5	*Wf3*	8
Lc2	7.5	*Wc1, Wc3*	9.5
Lc3	10.5	*Wc2*	8.5

Fig. 1, there are two horizontal L-C resonators (i.e., L_{hs}-C_{hs} and L_{hp}-C_{hp}) and two vertical L-C resonators (i.e., L_{vs}-C_{vs} and L_{vp}-C_{vp}). The total impedance of the horizontal branch and the total admittance of the vertical branch are given by (1) and (2), respectively:

$$Z_h = Z_{hs} + Z_{hp} = j\omega L_{hs} + \frac{1}{j\omega C_{hs}} + \frac{1}{j\omega C_{hp} + \frac{1}{j\omega L_{hp}}} \quad (1)$$

$$Y_v = Y_{vs} + Y_{vp} = \frac{1}{j\omega L_{vs} + \frac{1}{j\omega C_{vs}}} + j\omega C_{vp} + \frac{1}{j\omega L_{vp}} \quad (2)$$

The corresponding resonant frequency of each resonator is given by (3):

$$\omega_{hs} = \frac{1}{\sqrt{L_{hs}C_{hs}}},\ \omega_{hp} = \frac{1}{\sqrt{L_{hp}C_{hp}}},\ \omega_{vs} = \frac{1}{\sqrt{L_{vs}C_{vs}}},\ \omega_{vp} = \frac{1}{\sqrt{L_{vp}C_{vp}}} \quad (3)$$

The transmission ABCD matrix of an ECRLH TL unit cell can be given by (4):

$$\begin{bmatrix} A & B \\ C & D \end{bmatrix}_{1\_unit} = \begin{bmatrix} 1 & Z_h \\ 0 & 1 \end{bmatrix} \begin{bmatrix} 1 & 0 \\ Y_v & 1 \end{bmatrix} = \begin{bmatrix} 1 + Z_h Y_v & Z_h \\ Y_v & 1 \end{bmatrix} \quad (4)$$

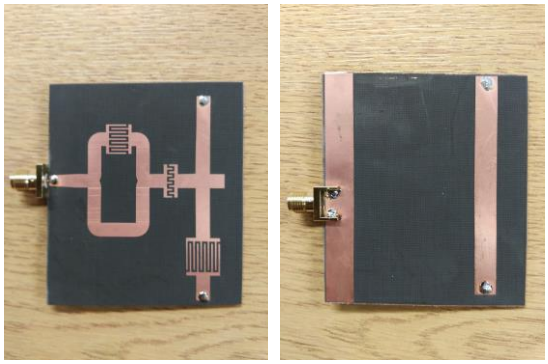

Fig. 4. Photographs of the fabricated antenna, (a) front view; (b) rear view.

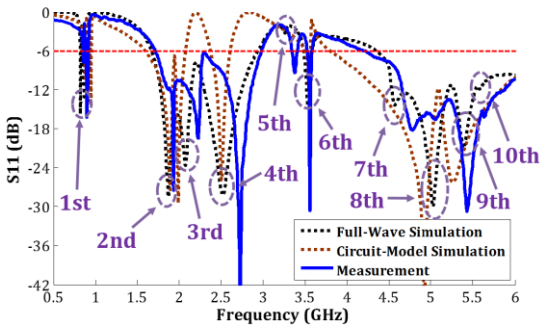

Fig. 5. Full-wave simulated, circuit-model simulated and measured S11 results of the proposed RA.

The ECRLH TL structure can mainly work at two different operating conditions - unbalanced and balanced condition [8]. In the unbalanced condition, there is a stopband in the transition area from the LH band to the RH band within each CRLH band. In the balanced condition, the original stopband within each CRLH band is closed to form the smooth transition from the LH band to the RH band. Thus, two balanced points are formed within both CRLH bands simultaneously. For the balanced condition, ω_0 is defined within the middle bandgap area, which is also the resonant frequency of L_{hp}-C_{hp} and L_{vs}-C_{vs}, i.e., $\omega_0 = \omega_{hp} = \omega_{vs}$ [8]. Different operating conditions of the metamaterial-based (e.g., CRLH or ECRLH) unit cell can result in different frequency responses of the RA. In [6], the effects of the operating conditions of one CRLH unit cell on the frequency response of a microstrip-fed monopole antenna loaded with this unit cell have been demonstrated. Benefiting from the characteristics of the unbalanced condition, the RAs usually designed with this metamaterial-based unit cell in this condition may generate multiple operating resonances working at the chosen frequencies.

III. SIMULATION AND MEASUREMENT

A. Antenna Design

The proposed RA is realized on *Rogers RT/duroid 5880* with thickness of 1.575 mm, dielectric constant of 2.2, and loss tangent of 0.0009. As shown in Fig. 2, this RA mainly includes an asymmetric ECRLH TL unit cell structure as the major radiator and a short microstrip line as the feeding line. The IDSs for C_{hs}, C_{hp}, and C_{vs} shown in Fig. 3 are designed in this RA structure. C_{vp} is achieved by the parasitic capacitance of the vertical parallel copper strips. These vertical paralleled strips

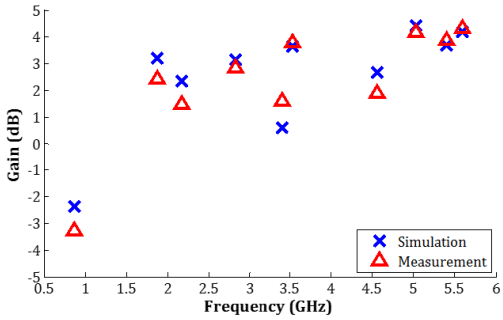

Fig. 6. Simulated and measured gains of the proposed RA at resonant frequencies.

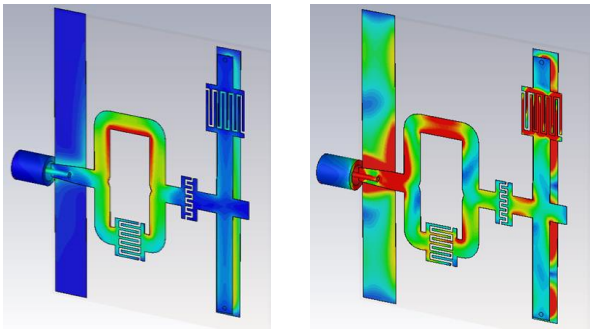

(a) (b)

Fig. 7. Current distribution of this RA at (a) 0.887 GHz; (b) 5.5 GHz.

are respectively placed on the top and bottom layers and are connected through two metalized vias. The metal strip on the bottom layer is modelled as the ground of the ECRLH unit cell, which is not connected to the main ground of the antenna. L_{hs}, L_{hp}, L_{vp} and L_{vs} are realized by the horizontal and vertical copper strips. The overall size of the proposed RA is 56 mm × 64 mm × 1.575 mm (i.e., $0.16\lambda_0 \times 0.18\lambda_0 \times 0.004\lambda_0$, where λ_0 is the wavelength of the lowest operating frequency of 0.887 GHz). The detailed dimensions of the proposed RA and three IDSs are listed in Table I. The photographs of the fabricated antenna are presented in Fig. 4.

B. Measurement and Simulation

The full-wave simulated (black dash line) and measured (blue solid line) S11 results of the proposed RA are shown in Fig. 5. According to the full-wave simulation, this RA has ten operating resonances over 0.5-6 GHz respectively working at GSM-850, DCS, PCS, UMTS, Bluetooth, WiFi (2.4 GHz and 5 GHz), TD-2500 and WiMAX (2500-2690 MHz, 3400-3690 MHz, and 5250-5280 MHz). Fig. 6 shows the measured and simulated gains of this RA. At 0.887 GHz, the simulated gain is -2.358 dB and the measured one is -3.38 dB. For the 1st operating resonance at 0.887 GHz, the current mainly flows around the loop structure formed by the parts of L_{hp} and C_{hp} in this RA structure, which is shown in Fig. 7(a). The electrically small size of this loop structure results in the low radiation efficiency, which further leads to the low antenna gain. However, the full-wave simulation shows that the radiation efficiency and antenna gain using this operating resonance will be improved at higher frequencies. Fig. 8 plots the measured and simulated co-polarized and cross-polarized radiation patterns of YOZ and XOY planes at 0.887 GHz, 2.4 GHz and

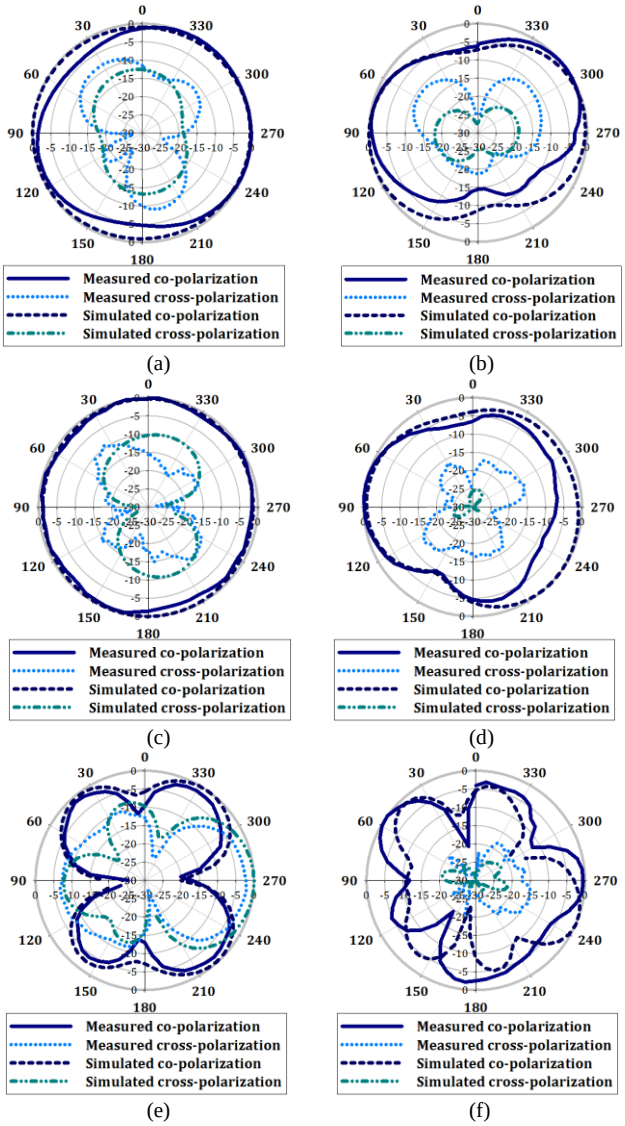

Fig. 8. Farfield patterns of the proposed RA, (a) YOZ plane at 0.887 GHz; (b) XOY plane at 0.887 GHz; (c) YOZ plane at 2.4 GHz; (d) XOY plane at 2.4 GHz; (e) YOZ plane at 5.5 GHz; (f) XOY plane at 5.5 GHz.

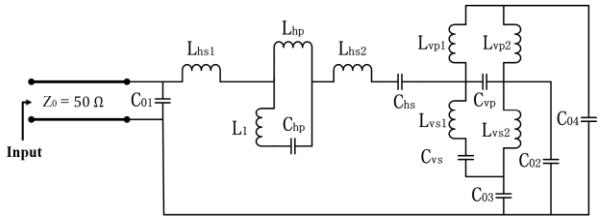

Fig. 9. Equivalent circuit model of the proposed RA.

5.5 GHz, respectively. The patterns at 0.887 GHz and 2.4 GHz are omnidirectional. However, the patterns at 5.5 GHz are non-omnidirectional, due to the radiation characteristics of a combination of multiple radiation parts (i.e., *L1*, *L2*, *L6*, *L7*, *W2*, and *Wf3*) in the RA structure as shown in Fig. 7 (b). According to Fig. 8 (b), Fig. 8(d) and Fig. 8(f), this RA exhibits the patterns with a horizontal linear electric field polarization.

C. Analysis of RA

The equivalent circuit model of the proposed RA is developed, which is shown in Fig. 9. In this model, C_{01}, C_{02},

TABLE II
COMPONENT VALUES IN THE EQUIVALENT CIRCUIT MODEL

Symbol	Values (pF)	Symbol	Values (nH)
C_{01}	0.35	L_{hs1}	1.2
C_{02}	0.32	L_{hs2}	2.8
C_{03}	0.25	L_{hp}	9.3
C_{04}	0.27	L_1	7.8
C_{hp}	1.7	L_{vs1}	6.2
C_{hs}	0.48	L_{vs2}	10.8
C_{vs}	1.9	L_{vp1}	11.1
C_{vp}	0.85	L_{vp2}	13.6

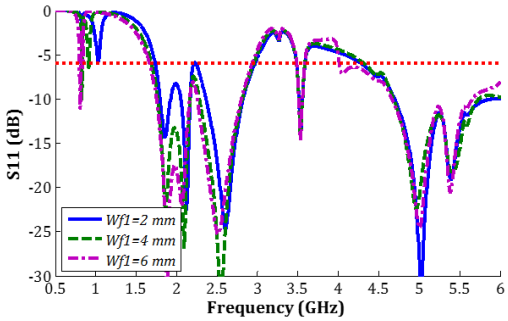

Fig. 10. Effects of the changing of the finger length *Wf1* for the IDS C_{hp} on the frequency response of the proposed RA.

TABLE III
SUMMARY OF MAJOR CONTROL PARTS AND PRIMARY RADIATION SOURCES FOR EACH OPERATING RESONANCE

No. of Resonance	Major Control Parts	Primary Radiation Sources
1st	*Wf1, W2,* and *W3*	Loop
2nd	*Wf2,* and *L1*	Ground
3rd	*Wf2* and *Wf3*	Dipole
4th	*Wf2, Wf3, L1,* and *L3*	Ground and dipole
5th	*Wf2, Wf3,* and *L3*	Ground and dipole
6th	*Wf3, L6,* and *L7*	Dipole
7th	*Wf2, L1, L3,* and *W3*	Ground and loop
8th	*L1, L3, L6, W2,* and *W3*	Ground, loop, and dipole
9th	*Wf3, L1, L2, L6, L7,* and *W2*	Ground, loop, and dipole
10th	*Wf3, L3, L6, L7, W2,* and *W3*	Ground, loop, and dipole

C_{03}, and C_{04} represent the parasitic capacitances between different parts of the ECRLH unit cell structure and the main ground. The parameter values are firstly extracted by analyzing each part of the antenna structure from the full-wave simulated data, and appropriate values are then selected for C_{01}, C_{02}, C_{03}, and C_{04}. After further optimization, the final component values extracted for the circuit model are listed in Table II. The circuit-model simulated S11 (brown dash line) is also shown in Fig. 5. The difference between the full-wave and circuit-model simulated S11 mainly results from the neglect of some coupling effects among the antenna structure which is for slight simplification of the equivalent model.

In terms of the operating resonances, each is generated by the specific parts of the RA structure. For instance, the 1st operating resonance mainly radiates and is controlled by the parts of *Wf1*, *W2* and *W3* of the loop structure. Fig. 10 shows that the finger length changing of *Wf1* mainly affects the 1st operating resonance with little influence on the coverage of the other operating resonances. The radiation and control of the other operating resonances can be also analyzed by investigating the current distribution at each corresponding resonant frequency. At each resonant frequency, the current distribution is intensive on the main ground, or the IDS-loaded loop structure, or the IDS-loaded dipole structure (i.e., mainly formed by the parts of L_{vs}, L_{vp}, C_{vs} and C_{vp}), or a combination of them. Table III summarizes the major parts in this RA structure that control each operating resonance and the primary radiation sources for each operating resonance. Thus, the proposed RA can be equivalently viewed as a complicated combination of a ground loop and dipole structures loaded with three IDSs.

IV. CONCLUSION

This letter proposes a microstrip-fed open-ended RA based on the ECRLH TL unit cell structure. This RA generates multiple operating resonances covering the commercial frequency bands of GSM-850, DCS, PCS, UMTS, Bluetooth, WiFi (2.4 GHz and 5 GHz), TD-2500 and WiMAX (2500-2690 MHz, 3400-3690 MHz, and 5250-5280 MHz). The equivalent circuit model of this antenna is further developed. The major control parts in the antenna structure and the primary radiation sources for each operating resonance are summarized. The exploration of independent control of one or some specific operating resonances and the radiation improvement of the 1st operating resonance will be taken as future research directions.

REFERENCES

[1] Yu-Jen Chi, and Fu-Chiarng Chen, "CRLH Leaky Wave Antenna Based on ACPS Technology With 180° Horizontal Plane Scanning Capability," *IEEE Trans. Antennas Propag.*, vol. 61, pp. 571 – 577, Feb. 2013.

[2] Dong-Jin Kim, and Jeong-Hae Lee, "Beam Scanning Leaky-Wave Slot Antenna Using Balanced CRLH Waveguide Operating Above the Cutoff Frequency," *IEEE Trans. Antennas Propag.*, vol. 61, pp. 2432 – 2440, May 2013.

[3] Amir Ali Tavallaee, Philip W. C. Hon, Karan Mehta, Tatsuo Itoh, and Benjamin S. Williams, "Zero-Index Terahertz Quantum-Cascade Metamaterial Lasers," *IEEE Journal of Quantum Electronics*, Vol. 46, , pp. 1091 – 1098, Jul. 2010.

[4] Pei-Ling Chi, and Yi-Sen Shih, "Compact and Bandwidth-Enhanced Zeroth-Order Resonant Antenna," *IEEE Antenna Wireless Propag. Lett.*, vol. 14, pp. 285 - 288, 2015.

[5] Hong-Min Lee, "A Compact Zeroth-Order Resonant Antenna Employing Novel Composite Right/Left-Handed Transmission-Line Unit-Cells Structure," *IEEE Antenna Wireless Propag. Lett.*, vol. 10, pp. 1377 - 1380, 2011.

[6] Amr A. Ibrahim, and Amr M. E. Safwat, "Triple-Band Microstrip-Fed Monopole Antenna Loaded with CRLH Unit Cell," *IEEE Antenna Wireless Propag. Lett.*, vol. 10, pp. 1547 – 1550, Dec. 2011.

[7] A. Rennings, S. Otto, J. Mosig, C. Caloz, and I. Wolff, "Extended Composite Right/Left-Handed (E-CRLH) Metamaterial and its Application as Quad-band Quarter-Wavelength Transmission Line", *Proc. of Asia-Pacific Microwave Conf.*, pp. 1405 – 1408, 2006.

[8] G. V. Eleftheriades, "Design of generalized negative refractive index transmission lines for quad-band applications", *IET Microw. Antennas Propag.*, Vol. 4, pp. 977 – 981, 2010.

[9] Rasool Keshavarz, Abbas Mohammadi, and Abdolali Abdipour, "A Quad-Band Distributed Amplifier with E-CRLH Transmission Line", *IEEE Trans. Microw. Theory Tech.*, vol. 61, no. 12, pp. 4188 – 4194, Dec. 2013.

[10] Miguel Durán-Sindreu, Jun Choi, Jordi Bonache, Ferran Martín, and Tatsuo Itoh, "Dual-band leaky wave antenna with filtering capability based on extended-composite right/left-handed transmission lines", *Microwave Symposium Digest (IMS), 2013 IEEE MTT-S International*, Seattle, WA, pp. 1- 4, June 2013.